



TENSILE/COMPRESSIVE RESPONSE OF 316L STAINLESS STEEL FABRICATED BY ADDITIVE MANUFACTURING

RESPUESTA A LA TENSIÓN/COMPRESIÓN DEL ACERO INOXIDABLE 316L FABRICADO POR MANUFACTURA ADITIVA

Germán Omar Barrionuevo^{1,*}, Iván La Fé-Perdomo^{2,3}, Esteban Cáceres-Brito¹, Wilson Navas-Pinto^{1,4}

Received: 01-10-2023, Received after review: 28-11-2023, Accepted: 12-12-2023, Published: 01-01-2024

Abstract

Additive manufacturing has evolved from a rapid prototyping technology to a technology with the ability to produce highly complex parts with superior mechanical properties than those obtained conventionally. The processing of metallic powders by means of a laser makes it possible to process any type of alloy and even metal matrix composites. The present work analyzes the tensile and compressive response of 316L stainless steel processed by laser-based powder bed fusion. The resulting microstructure was evaluated by optical microscopy. Regarding the mechanical properties, the yield strength, ultimate tensile strength, percentage of elongation before breakage, compressive strength and microhardness were determined. The results show that the microstructure is constituted by stacked micro molten pools, within which cellular sub-grains are formed due to the high thermal gradient and solidification rate. The compressive strength (1511.88 ± 9.22 MPa) is higher than the tensile strength (634.80 ± 11.62 MPa). This difference is mainly associated with strain hardening and the presence of residual stresses. The initial microhardness was 206.24 ± 11.96 HV; after the compression test, the hardness increased by 23%.

Keywords: Additive manufacturing, Laser powder bed fusion, Mechanical properties, Stainless steel, Strain hardening

Resumen

La manufactura aditiva pasó de ser una tecnología de prototipado rápido a una tecnología con la capacidad de producir piezas de gran complejidad y con propiedades mecánicas superiores a las obtenidas convencionalmente. El procesamiento de polvos metálicos a través de un láser permite procesar cualquier tipo de aleación e incluso materiales compuestos. En el presente trabajo se analiza la respuesta a tracción y compresión del acero inoxidable 316L procesado mediante fusión selectiva láser. Se analizó la microestructura resultante mediante microscopía óptica; respecto a las propiedades mecánicas se determinó la resistencia a la fluencia, resistencia última a la tracción, porcentaje de elongación antes de la rotura, resistencia a la compresión y microdureza. Los resultados obtenidos muestran que la microestructura está constituida por micropiletas fundidas apiladas, dentro de las cuales se generan subgranos celulares, producto del elevado gradiente térmico y la alta tasa de solidificación. La resistencia a la compresión (1511.88 ± 9.22 MPa) es mayor a la resistencia a tracción (634.80 ± 11.62 MPa). Esta diferencia está asociada principalmente al endurecimiento por deformación y la presencia de esfuerzos residuales. La microdureza inicial fue de 206.24 ± 11.96 HV; posterior al ensayo de compresión la dureza se incrementó un 23%.

Palabras clave: manufactura aditiva, fusión selectiva láser, propiedades mecánicas, acero inoxidable, endurecimiento por deformación

^{1,*}Departamento de Ciencias de la Energía y Mecánica, Universidad de las Fuerzas Armadas ESPE, Quito, Ecuador.
Corresponding author ✉: gobarrionuevo@uc.cl.

²Departamento de Ingeniería Mecánica y Metalúrgica, Escuela de Ingeniería, Pontificia Universidad Católica de Chile, Santiago, Chile.

³Study Centre on Advanced and Sustainable Manufacturing, University of Matanzas, Matanzas, Cuba

⁴Department of Mechanical Engineering, University of Saskatchewan, Saskatoon, Canada.

Suggested citation: Barrionuevo, G.O.; La Fé-Perdomo, I.; Cáceres-Brito, E.; Navas-Pinto, W. "Tensile/Compressive Response of 316L Stainless Steel Fabricated by Additive Manufacturing," *Ingenius, Revista de Ciencia y Tecnología*, N.º 31, pp. 9-18, 2024, DOI: <https://doi.org/10.17163/ings.n31.2024.01>.

1. Introduction

Additive manufacturing (AM) technology emerged as a rapid prototyping technique. Although initially focused on polymer processing with techniques such as stereolithography (SLA) and fused deposition modeling (FDM) in the 1980s, it was later extended to the processing of metals, ceramics, and composites [1, 2].

AM came from the minds of two chemical engineers who developed a toy for their daughter, which deposited a polymer layer by layer [3]. They patented their invention in 1986. A few years later, they consolidated one of the most successful additive manufacturing companies to date, Stratasy. Already in the 1990s, the first developments in metal processing appeared, with technologies such as selective laser melting (SLM) and selective laser sintering (SLS) [4, 5]. It is worth noting that all these developments went hand in hand with universities and research centers, which accelerated technological development.

The last few years have seen great advances in processing various types of materials [6]. Manufacturers have expanded their product portfolio to include equipment, raw materials, and consumables. In addition, extensive research has been developed to investigate the potential benefits of AM in different fields. For instance, several opportunities as possible cost and lead time reductions, the possibility of unique design solutions, and the consolidation of multiple components, have been identified [7]. However, additive manufacturing is not yet a plug-and-play technology. It requires a thorough knowledge of the material to be processed, suitable processing parameters, and environmental conditions, among others [5]. Furthermore, AM also requires substantial work and research in order to obtain diverse certifications and standards required in different fields to demonstrate its efficiency in manufacturing complex parts and assure their repeatability and quality [7].

FDM technology is one of the most widely used technologies, mainly due to its ease of installation and work [8–11]. In contrast, metal fabrication requires expensive and more complex equipment. Metal AM is classified into directed energy deposition (DED) [12–14] and powder bed fusion (PBF) [15, 16]; within DED, the technology that stands out for its versatility and processing capability is wire arc additive manufacturing (WAAM) [17–20]. On the other hand, in PBF, the best option for the manufacture of parts of great geometric complexity and reduced size is laser-based powder bed fusion (LPBF) [21].

LPBF uses a medium-power laser (100-400 W) to melt metal powders, which change phase in microseconds, creating repetitive cycles of melting and solidification that produce microstructures never seen before [22, 23]. One of the notable features is the formation of smaller grains compared to the same material

processed conventionally. In addition, micro-molten pools are created within which cellular subgrains are formed. These peculiar microstructures give rise to different mechanical properties [?, 24], which require multiple mechanical tests to determine their suitability for use as load-bearing structural elements or in dynamic environments under varying loads.

Regarding the mechanical properties, a significant improvement in different mechanical properties of specimens manufactured by means of LPBF has been observed. For instance, Röttger et al. [25] compared the mechanical properties of specimens manufactured with 316L austenitic steel processed by SLM technology and specimens manufactured through a regular casting process. After performing tensile tests, it was observed that the tensile strength increased by approximately 20 % in samples produced by AM. Moreover, Kurzynowski et al. [26] carried out tensile tests on 316L stainless steel specimens manufactured by SLM with different process parameters and compared the results with the mechanical properties of samples made from rolled sheet AISI SS316L. An improvement in the yield strength and Young's modulus was observed after testing. In addition, Liverani et al. [27] studied the effect of different process parameters on the microstructure and mechanical properties of specimens produced by SLM. After performing tensile and fatigue tests, the experimental results suggest the possibility of an improvement of the ultimate tensile strength and the percentage of elongation of the specimens when compared to conventionally manufactured AISI316L samples. In a different study, Liverani et al. [28] reported a yield strength (σ_Y) of around 400 MPa and an ultimate tensile strength (σ_{UTS}) between 500-600 MPa. Larimian et al. [29] obtained similar results, highlighting the effect of processing parameters and the scanning strategy on the resulting strength. The lowest and highest σ_Y was 148 and 462 MPa, respectively. While, the σ_{UTS} values were around 178 and 584 MPa. It is worth noting that to obtain an adequate mechanical response, it is essential to obtain samples with the maximum relative density.

In the case of compressive response, Güden et al. [30] investigated the influence of the strain rate during compression tests of selective laser melted 316L stainless steel and reported ultimate true compression stresses in the range of 1400 to 1600 MPa with strain rates ranging from 2800 to 3250 s^{-1} , respectively. Li et al. [31] developed a constitutive model to predict the compressive stress-strain of 316L stainless steel processed by LPBF and compared the results with specimens manufactured with SLM equipment at different scanning speeds. An average compressive stress of 1400 MPa and a strain of 23 % were obtained.

Therefore, the present work is focused on determining the tensile and compressive response of 316L stainless steel processed by laser powder bed fusion technol-

ogy under specific conditions. As the microstructure plays a fundamental role in comprehending the resulting mechanical properties, an in-depth analysis is carried out of the microstructural features as well as the relative density.

2. Materials and Methods

The material used to fabricate the samples was 316L stainless steel, whose nominal chemical composition is detailed in Table 1.

Table 1. Nominal chemical composition of the AISI 316L stainless steel powders.

Elements (wt%)				
Fe	Cr	Ni	Mo	Mn
Bal.	16.5-18	10-13	2-2.5	0-2
	Si	C	P	S
	0-1	0-0.03	0-0.04	0-0.03

The selective laser melting process was carried out in a Concept Laser machine (MLAB 200R) equipped with a 200W fiber laser (Nb:YAG) with a wavelength of 1064 nm. The powders were deposited on a 16 mm thick 316L stainless-steel support plate. The processing parameters were a laser power of 160 W, a scanning speed of 800 mm/s, hatch spacing of 60 μm and a layer thickness of 30 μm (Figure 1); these parameters were chosen to maximize the relative density, reducing the porosity of the printed samples.

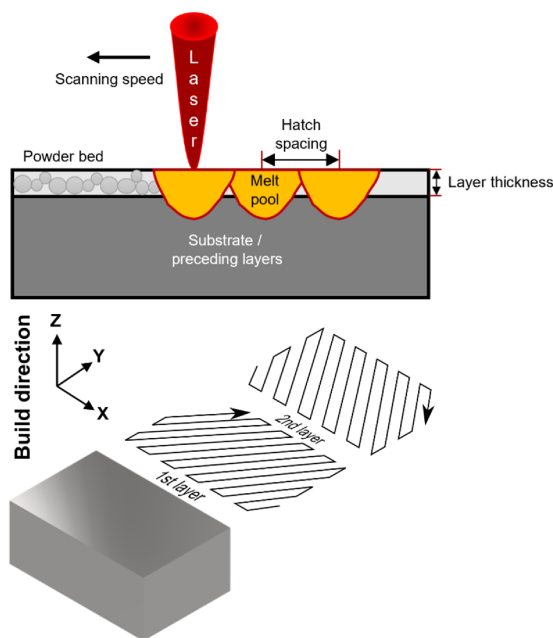


Figure 1. Schematic representation of the laser-based powder bed fusion process, identifying the key processing parameters and the scanning strategy.

Flat dog-bone geometry specimens agreeing to ASTM E8/8M-21 and prismatic samples of 16x10x7

mm were fabricated with a meander scanning strategy with a 67° rotation after each deposited layer. After manufacturing, all the samples were cut from the build platforms by wire-electrical discharge machining.

For the metallographic inspection, the samples were first planar ground using SiC paper, starting from 120 to 2000 grit to roughly polish the sample surface. Then, finely polished using alumina and posteriorly diamond paste. The material microstructure was revealed by chemical etching immersion in Aqua regia solution (20 ml HNO₃ and 60 ml HCl) for 30 s. The material surface morphology was inspected by means of optical microscopy (OM) (MEIJI IM 7200). The OM micrographs were processed and analyzed using Fiji software (National Institutes of Health, USA) to determine microstructural features and evaluate porosity by means of image analysis.

Tensile tests following the ASTM E8/8M-21 were carried out using a universal tensile tester machine (Instron 3368, Zwick) with a 50 kN load cell and a 2 mm/min speed to fracture and a gauge length of 50 mm with an extensometer. According to ASTM E9-09, compressive tests were carried out using the prismatic specimens. Four prismatic specimens were tested, and the average results were reported. In addition, the elastic modulus was calculated according to ASTM E111.

Microhardness was measured using a Vickers hardness tester (METKON DUROLINE-M), using a 500 g force and 10 s as dwell time, according to ASTM E384 standard. Mean values were recorded through five measurements and then reported.

3. Results and discussion

Figure 2 shows the manufactured test specimens. It is worth noting that both the powder and the support plate must be manufactured from the same material to obtain proper adhesion between the two parts and avoid errors or displacements during the additive manufacturing process.



Figure 2. Additively manufactured samples for microstructure and mechanical evaluation. Base plate dimension: 100 x 100 x 16 mm.

In order to determine the relative density, the surface defects obtained by optical microscopy were evaluated (Figure 3). By means of image analysis, a relative density of 99.7 % was obtained.

Obtaining parts with a relative density greater than 99 % is essential to obtain comparable mechanical properties to parts manufactured by conventional methods. As can be seen in Figure 3, there are still circular porosities, which are associated with the gas trapped inside the metal powder [32]. However, most of the surface is free of pores, which ensures the suitable performance of the manufactured samples and the proper selection of the chosen processing parameters.

3.1. Microstructure analysis

Figure 4 presents the 3D assembly of optical micrographs obtained in different manufacturing planes. It is possible to appreciate that the scanning strategy used can be distinguished in the upper plane. At the same time, it is possible to observe the stacking of micro-molten pools in the lateral planes. Figure 5a shows in more detail the arrangement of molten pools, where it is possible to extract that, on average, the molten pool has a depth of approximately $50\ \mu\text{m}$ and an extension of $140\ \mu\text{m}$. Figure 5b shows the detail of a molten pool within which cellular sub-grains appear, as reported in previous research work [33–36].

Cellular grains can be distinguished within the molten pool (Figure 5b); these sub-grains are produced due to the high thermal gradient and solidification rate [37]. As the fusion-solidification process is generated layer by layer, the molten pool deforms slightly due to the presence of residual stresses [38, 39]. The scanning strategy also causes the molten pool to deform; the rotation of the printing angle modifies the thermal gradient, modifying the geometry of the micro molten pools.

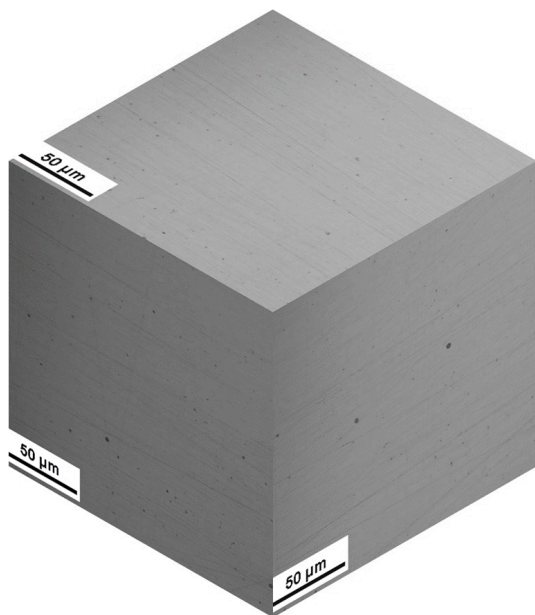
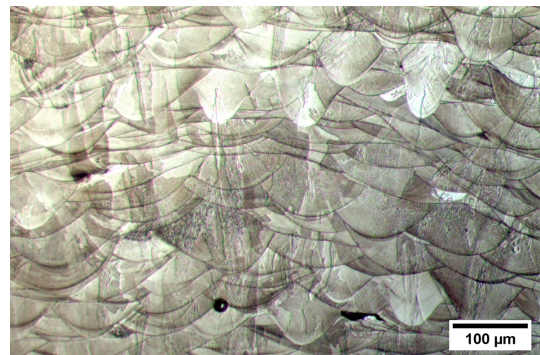


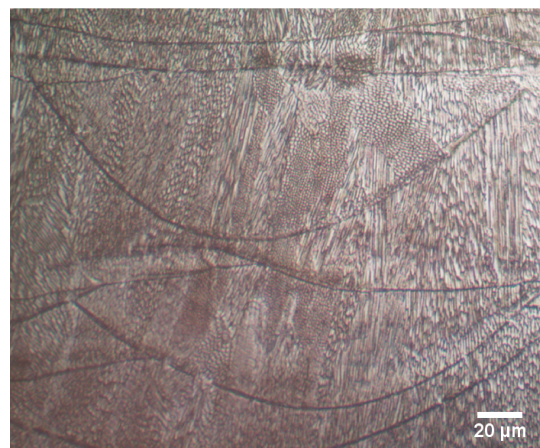
Figure 3. Optical micrograph to assess the internal porosity.



Figure 4. 3D assembly of optical micrographs of the 316 L stainless steel processed by LPBF.



(a)



(b)

Figure 5. Optical micrograph of the additively processed 316L stainless steel a) 200x, b) 1000x highlighting the molten pool.

3.2. Mechanical response

Figure 6 shows the stress-strain curve of 316L stainless steel subjected to a tensile test. The yield stress was 512.32 ± 7.84 MPa, the ultimate tensile stress was 634.80 ± 11.62 MPa, and the deformation before rupture was 31.61 ± 1.40 %.

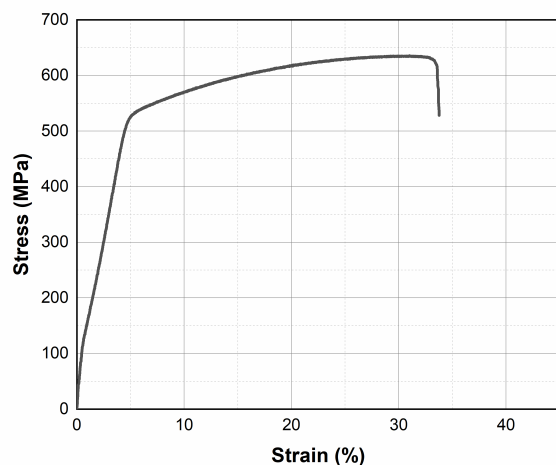


Figure 6. Tensile evaluation of LPBF 316L stainless steel.

As can be seen in Figure 6, the material shows a ductile response with a large deformation after exceeding the elastic limit region. In addition, the yield strength for the material has been determined to be around 512.32 MPa, corresponding to an engineering strain of 0.05. Accordingly, the ultimate tensile strength is around 634.80 MPa at a strain of approximately 0.32. For the manufactured group of specimens, the elastic modulus was determined to be around 229.12 ± 2.14 GPa. In addition, once the plastic deformation has begun, it is possible to observe a stable strain hardening stage followed by a necking region that leads to the fracture of the specimen. Even though the ductile response is associated with the absence of porosity, if there is a low relative density, the material tends to fracture in a brittle manner [40] due to the presence of defects such as trapped gas, unstable melting pools or lack of fusion [41].

Figure 7 shows the necking that occurs in the sample before breakage. The necking and area reduction is a typical indicator of the ductile response of the tested material. Additionally, it can be observed that the fracture occurs at an angle of about 45° .

The failure mechanism of 316L stainless steel fabricated by additive manufacturing may be associated with the microvoid coalescence fracture, which occurs when the material contains small pores or inclusions that grow and coalesce under tensile stress, forming internal microcracks.

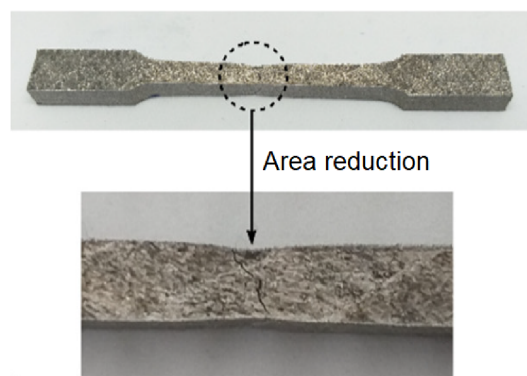


Figure 7. Area reduction of the specimen used in the tensile test.

Figure 8 shows the compressive response of the additively manufactured stainless steel specimens. The compressive strength (1511.88 ± 9.22 MPa) is higher than the tensile strength (634.80 ± 11.62 MPa). This difference is mainly associated with strain hardening and residual stresses [?, 38], [42]. As can be seen in Figure 8, when the stress exceeds 500 MPa, the material starts to harden. Strain hardening makes the material capable of withstanding high stresses before failure occurs. In addition, the crystalline structure of austenitic stainless steel (FCC) typically contains planes of atoms that can slide past each other more easily under shear forces (such as in compression) than they can be pulled apart under tensile forces. In other words, the crystal structure of the 316L SS is more resistant to compression and shear forces.

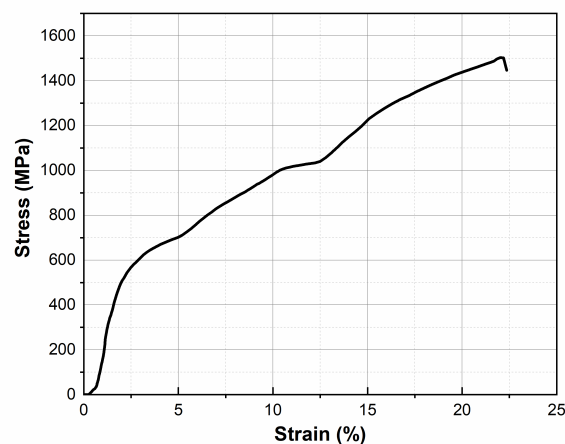


Figure 8. Compressive response of LPBF 316L stainless steel.

When subjected to compressive stress, the deformation of the material causes strain hardening. Therefore, the hardness was evaluated before and after the compression test (Figure 9).

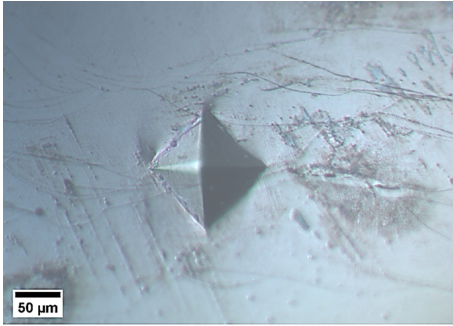


Figure 9. Microhardness evaluation of the 316L stainless steel processed by LPBF.

The initial microhardness was $206.24 \pm 11.96HV_{0.5}$ in the as-built condition. After the compression test, microhardness increases to $253.32 \pm 11.12HV_{0.5}$.

Figure 10 shows the deformation produced after the compression test, where it is evident how the molten pools have been deformed. The compression process acts as a strain-hardening treatment. It has been observed that the molten pools are deformed, which generates a kind of cold working treatment. Internally, the grains are compressed, reducing their size, which increases the hardness. The microhardness has increased by 23 %.

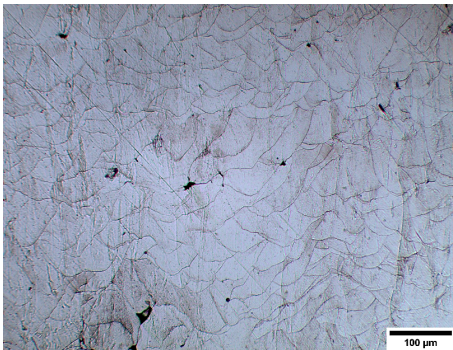


Figure 10. Compressed molten pools after compression test.

Table 2 summarizes the mechanical response of additively manufactured 316L stainless steel. The results obtained in the present work coincide with those reported in the literature [24], [25], [27], [29], [31], [40]. Therefore, it is possible to affirm that the SLM technology is reaching maturity, and work should begin on standards for its approval.

The tensile and compressive response of 316L stainless steel processed by SLM showed a mechanical response above its conventionally processed counterpart [24]. The higher strength is attributed to the microstructure. Within the molten pool, sub-grains of less than one micron were found due to the high thermal gradient resulting from the cyclic laser's interaction with the metal powders.

Additive manufacturing has a number of advantages in terms of design and flexibility. However, to ensure its use in engineering applications, it is necessary to further study its mechanical properties by varying process parameters and scanning strategies.

Table 2. Mechanical properties of the AISI 316L stainless steel additively manufactured.

Properties	Value
Yield strength (MPa)	512.32 ± 7.84
Tensile strength (MPa)	634.80 ± 11.62
Elastic modulus (GPa)	229.12 ± 2.14
Compressive strength (MPa)	1511.88 ± 9.22
Elongation (%)	31.61 ± 1.40
Microhardness (HV)	206.24 ± 11.96

4. Conclusions

In the present work, the tensile and compressive response of laser-processed 316L stainless steel has been evaluated. The main conclusions drawn are detailed below:

- Proper selection of processing parameters is essential to obtain parts with minimum porosity. The higher the relative density, the higher the mechanical properties, as the pores act as stress concentrators, reducing the mechanical strength. In this work, a relative density of 99.7 % was obtained.
- Additive manufacturing offers the possibility to control the microstructure and thus to customize certain mechanical properties. For example, the dimensions of the molten pool or the relative density. It is worth noting that the scanning strategy and the specimen geometry affect the thermal gradient and, thus, the resulting microstructure. Further research on these parameters and their effect on the mechanical properties is needed.
- Tensile and compression tests showed a ductile performance of the material obtained additively. In the case of the tensile test, the following results were obtained: a yield strength of 512.32 ± 7.84 MPa, an ultimate tensile strength of 635 MPa, and an elastic modulus of 229.12 ± 2.14 GPa. In addition, the stress-strain curve shows a ductile response of the material, which is associated with a high relative density and low porosity.

- A compressive strength of approximately 1511.88 \pm 9.22 MPa was observed in the corresponding tests. The significant difference between the tensile and compression response could be attributed to the presence of residual stress produced during the manufacturing process and a strain hardening mechanism caused by the deformation of the sample and confirmed by the distortion observed in the molten pools after the compression test was performed.
- The microhardness test confirmed an increase of approximately 23 % in the results obtained after a specimen was subjected to a compression test in contrast to the results of the specimens as manufactured.

References

- [1] N. Li, S. Huang, G. Zhang, R. Qin, W. Liu, H. Xiong, G. Shi, and J. Blackburn, "Progress in additive manufacturing on new materials: A review," *Journal of Materials Science & Technology*, vol. 35, no. 2, pp. 242–269, 2019, recent Advances in Additive Manufacturing of Metals and Alloys. [Online]. Available: <https://doi.org/10.1016/j.jmst.2018.09.002>
- [2] T. J. Gordelier, P. R. Thies, L. Turner, and L. Johanning, "Optimising the FDM additive manufacturing process to achieve maximum tensile strength: a state-of-the-art review," *Rapid Prototyping Journal*, vol. 25, no. 6, pp. 953–971, Jan 2019. [Online]. Available: <https://doi.org/10.1108/RPJ-07-2018-0183>
- [3] T. J. Wallin, J. H. Pikul, S. Bodkhe, B. N. Peele, B. C. Mac Murray, D. Therriault, B. W. McEnerney, R. P. Dillon, E. P. Giannelis, and R. F. Shepherd, "Click chemistry stereolithography for soft robots that self-heal," *J. Mater. Chem. B*, vol. 5, pp. 6249–6255, 2017. [Online]. Available: <http://dx.doi.org/10.1039/C7TB01605K>
- [4] C.-m. Liu, H.-b. Gao, L.-y. Li, J.-d. Wang, C.-h. Guo, and F.-c. Jiang, "A review on metal additive manufacturing: modeling and application of numerical simulation for heat and mass transfer and microstructure evolution," *China Foundry*, vol. 18, no. 4, pp. 317–334, Jul 2021. [Online]. Available: <https://doi.org/10.1007/s41230-021-1119-2>
- [5] N. Haghdadadi, M. Laleh, M. Moyle, and S. Primig, "Additive manufacturing of steels: a review of achievements and challenges," *Journal of Materials Science*, vol. 56, no. 1, pp. 64–107, Jan 2021. [Online]. Available: <https://doi.org/10.1007/s10853-020-05109-0>
- [6] K. R. Ryan, M. P. Down, and C. E. Banks, "Future of additive manufacturing: Overview of 4D and 3D printed smart and advanced materials and their applications," *Chemical Engineering Journal*, vol. 403, p. 126162, 2021. [Online]. Available: <https://doi.org/10.1016/j.cej.2020.126162>
- [7] B. Blakey-Milner, P. Gradl, G. Snedden, M. Brooks, J. Pitot, E. Lopez, M. Leary, F. Berto, and A. du Plessis, "Metal additive manufacturing in aerospace: A review," *Materials & Design*, vol. 209, p. 110008, 2021. [Online]. Available: <https://doi.org/10.1016/j.matdes.2021.110008>
- [8] M. Vishwas and C. Basavaraj, "Studies on optimizing process parameters of fused deposition modelling technology for ABS," *Materials Today: Proceedings*, vol. 4, no. 10, pp. 10994–11003, 2017, advanced Materials, Manufacturing, Management and Thermal Science (AMMMT 2016) September 23-24, 2016. [Online]. Available: <https://doi.org/10.1016/j.matpr.2017.08.057>
- [9] Z. Liu, Y. Wang, B. Wu, C. Cui, Y. Guo, and C. Yan, "A critical review of fused deposition modeling 3D printing technology in manufacturing polylactic acid parts," *The International Journal of Advanced Manufacturing Technology*, vol. 102, no. 9, pp. 2877–2889, Jun 2019. [Online]. Available: <https://doi.org/10.1007/s00170-019-03332-x>
- [10] G. O. Barrionuevo and J. A. Ramos-Grez, "Machine learning for optimizing technological properties of wood composite filament-timberfill fabricated by fused deposition modeling," in *Applied Technologies*, M. Botto-Tobar, M. Zambrano Vizueté, P. Torres-Carrión, S. Montes León, G. Pizarro Vásquez, and B. Durakovic, Eds. Cham: Springer International Publishing, 2020, pp. 119–132. [Online]. Available: https://doi.org/10.1007/978-3-030-42520-3_10
- [11] J. Chacón, M. Caminero, E. García-Plaza, and P. Núñez, "Additive manufacturing of PLA structures using fused deposition modelling: Effect of process parameters on mechanical properties and their optimal selection," *Materials & Design*, vol. 124, pp. 143–157, 2017. [Online]. Available: <https://doi.org/10.1016/j.matdes.2017.03.065>
- [12] A. Saboori, D. Gallo, S. Biamino, P. Fino, and M. Lombardi, "An overview of additive manufacturing of titanium components by directed energy deposition: Microstructure and mechanical properties," *Applied Sciences*, vol. 7, no. 9, 2017. [Online]. Available: <https://doi.org/10.3390/app7090883>
- [13] Z. Xia, J. Xu, J. Shi, T. Shi, C. Sun, and D. Qiu, "Microstructure evolution and

- mechanical properties of reduced activation steel manufactured through laser directed energy deposition,” *Additive Manufacturing*, vol. 33, p. 101114, 2020. [Online]. Available: <https://doi.org/10.1016/j.addma.2020.101114>
- [14] S. Gao, R. Liu, R. Huang, X. Song, and M. Seita, “A hybrid directed energy deposition process to manipulate microstructure and properties of austenitic stainless steel,” *Materials & Design*, vol. 213, p. 110360, 2022. [Online]. Available: <https://doi.org/10.1016/j.matdes.2021.110360>
- [15] G. O. Barrionuevo, M. Walczak, J. Ramos-Grez, and X. Sánchez-Sánchez, “Microhardness and wear resistance in materials manufactured by laser powder bed fusion: Machine learning approach for property prediction,” *CIRP Journal of Manufacturing Science and Technology*, vol. 43, pp. 106–114, 2023. [Online]. Available: <https://doi.org/10.1016/j.cirpj.2023.03.002>
- [16] S. Chowdhury, N. Yadaiah, C. Prakash, S. Ramakrishna, S. Dixit, L. R. Gupta, and D. Buddhi, “Laser powder bed fusion: a state-of-the-art review of the technology, materials, properties & defects, and numerical modelling,” *Journal of Materials Research and Technology*, vol. 20, pp. 2109–2172, 2022. [Online]. Available: <https://doi.org/10.1016/j.jmrt.2022.07.121>
- [17] S. W. Williams, F. Martina, A. C. Addison, G. P. J. Ding, and P. Colegrove, “Wire + arc additive manufacturing,” *Materials Science and Technology*, vol. 32, no. 7, pp. 641–647, 2016. [Online]. Available: <https://doi.org/10.1179/1743284715Y.0000000073>
- [18] W. Jin, C. Zhang, S. Jin, Y. Tian, D. Wellmann, and W. Liu, “Wire arc additive manufacturing of stainless steels: A review,” *Applied Sciences*, vol. 10, no. 5, 2020. [Online]. Available: <https://doi.org/10.3390/app10051563>
- [19] J. L. Z. Li, M. R. Alkahari, N. A. B. Rosli, R. Hasan, M. N. Sudin, and F. R. Ramli, “Review of wire arc additive manufacturing for 3D metal printing,” *International Journal of Automation Technology*, vol. 13, no. 3, pp. 346–353, 2019. [Online]. Available: <https://doi.org/10.20965/ijat.2019.p0346>
- [20] T. A. Rodrigues, V. Duarte, R. M. Miranda, T. G. Santos, and J. P. Oliveira, “Current status and perspectives on wire and arc additive manufacturing (WAAM),” *Materials*, vol. 12, no. 7, 2019. [Online]. Available: <https://doi.org/10.3390/ma12071121>
- [21] X. Zhang, C. J. Yocom, B. Mao, and Y. Liao, “Microstructure evolution during selective laser melting of metallic materials: A review,” *Journal of Laser Applications*, vol. 31, no. 3, p. 031201, May 2019. [Online]. Available: <https://doi.org/10.2351/1.5085206>
- [22] W. M. Tucho, V. H. Lysne, H. Austbø, A. Sjolyst-Kverneland, and V. Hansen, “Investigation of effects of process parameters on microstructure and hardness of SLM manufactured SS316L,” *Journal of Alloys and Compounds*, vol. 740, pp. 910–925, 2018. [Online]. Available: <https://doi.org/10.1016/j.jallcom.2018.01.098>
- [23] M. Tang, L. Zhang, and N. Zhang, “Microstructural evolution, mechanical and tribological properties of TiC/Ti6Al4V composites with unique microstructure prepared by SLM,” *Materials Science and Engineering: A*, vol. 814, p. 141187, 2021. [Online]. Available: <https://doi.org/10.1016/j.msea.2021.141187>
- [24] J. Fu, S. Qu, J. Ding, X. Song, and M. Fu, “Comparison of the microstructure, mechanical properties and distortion of stainless steel 316 l fabricated by micro and conventional laser powder bed fusion,” *Additive Manufacturing*, vol. 44, p. 102067, 2021. [Online]. Available: <https://doi.org/10.1016/j.addma.2021.102067>
- [25] W. H. Kan, L. N. S. Chiu, C. V. S. Lim, Y. Zhu, Y. Tian, D. Jiang, and A. Huang, “A critical review on the effects of process-induced porosity on the mechanical properties of alloys fabricated by laser powder bed fusion,” *Journal of Materials Science*, vol. 57, no. 21, pp. 9818–9865, Jun 2022. [Online]. Available: <https://doi.org/10.1007/s10853-022-06990-7>
- [26] T. Kurzynowski, K. Gruber, W. Stopyra, B. Kuznicka, and E. Chlebus, “Correlation between process parameters, microstructure and properties of 316L stainless steel processed by selective laser melting,” *Materials Science and Engineering: A*, vol. 718, pp. 64–73, 2018. [Online]. Available: <https://doi.org/10.1016/j.msea.2018.01.103>
- [27] E. Liverani, S. Toschi, L. Ceschini, and A. Fortunato, “Effect of selective laser melting (SLM) process parameters on microstructure and mechanical properties of 316L austenitic stainless steel,” *Journal of Materials Processing Technology*, vol. 249, pp. 255–263, 2017. [Online]. Available: <https://www.sciencedirect.com/science/article/pii/S0924013617302169>
- [28] E. Liverani, A. H. A. Lutey, A. Ascari, and A. Fortunato, “The effects of hot isostatic

- pressing (HIP) and solubilization heat treatment on the density, mechanical properties, and microstructure of austenitic stainless steel parts produced by selective laser melting (SLM),” *The International Journal of Advanced Manufacturing Technology*, vol. 107, no. 1, pp. 109–122, Mar 2020. [Online]. Available: <https://doi.org/10.1007/s00170-020-05072-9>
- [29] T. Larimian, M. Kannan, D. Grzesiak, B. Al-Mangour, and T. Borkar, “Effect of energy density and scanning strategy on densification, microstructure and mechanical properties of 316l stainless steel processed via selective laser melting,” *Materials Science and Engineering: A*, vol. 770, p. 138455, 2020. [Online]. Available: <https://doi.org/10.1016/j.msea.2019.138455>
- [30] M. Güden, S. Enser, M. Bayhan, A. Taşdemirci, and H. Yavaş, “The strain rate sensitive flow stresses and constitutive equations of a selective-laser-melt and an annealed-rolled 316l stainless steel: A comparative study,” *Materials Science and Engineering: A*, vol. 838, p. 142743, 2022. [Online]. Available: <https://doi.org/10.1016/j.msea.2022.142743>
- [31] Y. Li, Y. Ge, J. Lei, and W. Bai, “Mechanical properties and constitutive model of selective laser melting 316L stainless steel at different scanning speeds,” *Advances in Materials Science and Engineering*, vol. 2022, p. 2905843, Apr 2022. [Online]. Available: <https://doi.org/10.1155/2022/2905843>
- [32] B. Zhang, Y. Li, and Q. Bai, “Defect formation mechanisms in selective laser melting: A review,” *Chinese Journal of Mechanical Engineering*, vol. 30, no. 3, pp. 515–527, May 2017. [Online]. Available: <https://doi.org/10.1007/s10033-017-0121-5>
- [33] X. Ao, H. Xia, J. Liu, and Q. He, “Simulations of microstructure coupling with moving molten pool by selective laser melting using a cellular automaton,” *Materials & Design*, vol. 185, p. 108230, 2020. [Online]. Available: <https://doi.org/10.1016/j.matdes.2019.108230>
- [34] W. Yuan, H. Chen, T. Cheng, and Q. Wei, “Effects of laser scanning speeds on different states of the molten pool during selective laser melting: Simulation and experiment,” *Materials & Design*, vol. 189, p. 108542, 2020. [Online]. Available: <https://doi.org/10.1016/j.matdes.2020.108542>
- [35] P. Tang, H. Xie, S. Wang, X. Ding, Q. Zhang, H. Ma, J. Yang, S. Fan, M. Long, D. Chen, and X. Duan, “Numerical analysis of molten pool behavior and spatter formation with evaporation during selective laser melting of 316l stainless steel,” *Metallurgical and Materials Transactions B*, vol. 50, no. 5, pp. 2273–2283, Oct 2019. [Online]. Available: <https://doi.org/10.1007/s11663-019-01641-w>
- [36] G. O. Barrionuevo, J. Ramos-Grez, M. Walczak, and I. La Fé-Perdomo, “Numerical analysis of the effect of processing parameters on the microstructure of stainless steel 316L manufactured by laser-based powder bed fusion,” *Materials Today: Proceedings*, vol. 59, pp. 93–100, 2022, third International Conference on Recent Advances in Materials and Manufacturing 2021. [Online]. Available: <https://doi.org/10.1016/j.matpr.2021.10.209>
- [37] G. O. Barrionuevo, J. A. Ramos-Grez, M. Walczak, X. Sánchez-Sánchez, C. Guerra, A. Debut, and E. Haro, “Microstructure simulation and experimental evaluation of the anisotropy of 316L stainless steel manufactured by laser powder bed fusion,” *Rapid Prototyping Journal*, vol. 29, no. 3, pp. 425–436, Jan 2023. [Online]. Available: <https://doi.org/10.1108/RPJ-04-2022-0127>
- [38] H. Zhang, M. Xu, Z. Liu, C. Li, P. Kumar, Z. Liu, and Y. Zhang, “Microstructure, surface quality, residual stress, fatigue behavior and damage mechanisms of selective laser melted 304l stainless steel considering building direction,” *Additive Manufacturing*, vol. 46, p. 102147, 2021. [Online]. Available: <https://doi.org/10.1016/j.addma.2021.102147>
- [39] S. Mohanty, M. Arivarasu, N. Arivazhagan, and K. Phani Prabhakar, “The residual stress distribution of CO2 laser beam welded AISI 316 austenitic stainless steel and the effect of vibratory stress relief,” *Materials Science and Engineering: A*, vol. 703, pp. 227–235, 2017. [Online]. Available: <https://doi.org/10.1016/j.msea.2017.07.066>
- [40] I. La Fé-Perdomo, J. A. Ramos-Grez, I. Jeria, C. Guerra, and G. O. Barrionuevo, “Comparative analysis and experimental validation of statistical and machine learning-based regressors for modeling the surface roughness and mechanical properties of 316l stainless steel specimens produced by selective laser melting,” *Journal of Manufacturing Processes*, vol. 80, pp. 666–682, 2022. [Online]. Available: <https://doi.org/10.1016/j.jmapro.2022.06.021>
- [41] A. G. Amir Mahyar Khorasani, Ian Gibson and A. Ghaderi, “A comprehensive study on variability of relative density in selective laser melting of Ti-6Al-4V,” *Virtual and Physical Prototyping*, vol. 14, no. 4, pp. 349–359, 2019. [Online]. Available: <https://doi.org/10.1080/17452759.2019.1614198>

- [42] A. Eliasu, S. H. Duntu, K. S. Hukpati, M. Y. Amegadzie, J. Agyapong, F. Tetteh, A. Czekanski, and S. Boakye-Yiadom, “Effect of individual printing parameters on residual stress and tribological behaviour of 316L stainless steel fabricated with laser powder bed fusion (L-PBF),” *The International Journal of Advanced Manufacturing Technology*, vol. 119, no. 11, pp. 7041–7061, Apr 2022. [Online]. Available: <https://doi.org/10.1007/s00170-021-08489-y>